POLITECNICO DI TORINO
Repository ISTITUZIONALE

The other half of the sprinting coin: the neuromuscular profile of a 91-yr-old female world record sprinter

Original
The other half of the sprinting coin: the neuromuscular profile of a 91-yr-old female world record sprinter / Colosio, M., Dobrzycki, I., Teigen, L.E., Carbonaro, M., Ansaldo, M., Gatti, M., Brusco, C.M., Canepari, M., Bottinelli, R., Botter, A., Porcelli, S., Franchi, M.V., Sundberg, C.W.. - In: JOURNAL OF APPLIED PHYSIOLOGY. - ISSN 8750-7587. - STAMPA. - 140:6(2026), pp. 1605-1613. [10.1152/japplphysiol.00280.2026]

Availability:
This version is available at: 11583/3017237 since: 2026-10-30T16:27:14Z

Publisher:
APS

Published
DOI:10.1152/japplphysiol.00280.2026

Terms of use:

This article is made available under terms and conditions as specified in the corresponding bibliographic description in the repository

Publisher copyright

(Article begins on next page)

03 November 2026

american physiological society
JOURNAL OF APPLIED PHYSIOLOGY

J Appl Physiol 140: 1605–1613, 2026.
First published May 6, 2026; doi:10.1152/japplphysiol.00280.2026

SHORT REPORT

Experiments of Nature

The other half of the sprinting coin: the neuromuscular profile of a 91-yr-old female world record sprinter

Marta Colosio,[1,2] Isabell Dobrzycki,[2] Laura E. Teigen,[2] Marco Carbonaro,[3,4] Massimiliano Ansaldo,[1] Marco Gatti,[1] Clarissa Muller Brusco,[5] Monica Canepari,[1] Roberto Bottinelli,[1] Alberto Botter,[3] Simone Porcelli,[1,6] Martino V. Franchi,[5]* and Christopher W. Sundberg[2,7]*

[1]*Department of Molecular Medicine, University of Pavia, Pavia, Italy;* [2]*Division of Geriatrics and Gerontology, Department of Medicine, School of Medicine and Public Health, University of Wisconsin–Madison, Madison, Wisconsin, United States;* [3]*LISiN, Department of Electronics and Telecommunications, Politecnico di Torino, Torino, Italy;* [4]*Department of Biomechanical Engineering, University of Twente, Enschede, The Netherlands;* [5]*Department of Biomedical Sciences, Institute of Physiology, University of Padova, Padova, Italy;* [6]*Fondazione IRCCS Policlinico San Matteo, Pavia, Italy; and* [7]*Department of Kinesiology, School of Education, University of Wisconsin–Madison, Madison, Wisconsin, United States*

Abstract

A 91-yr-old female set the W90$^+$ world record in the 200 m sprint in 2024. We characterized her neuromuscular function, fatigability, denervation markers, and single-fiber contractile properties, and, where possible, compared these outcomes with published reference data. Knee extensor muscle architecture, force, power, fatigability, and motor unit (MU) behavior were assessed in vivo, and a vastus lateralis biopsy was analyzed for single-fiber contractile properties and markers of denervation. Quadriceps cross-sectional area was 36.5 cm^2, with fascicle length, pennation angle, and muscle thickness of 6.7 cm, 11.6°, and 1.4 cm, respectively. Knee extensor maximal voluntary isometric contraction (MVIC) torque was 79 Nm, power was 28 W, and power declined by 43% during a 4-min fatiguing task. MU recruitment threshold was 12 ± 11% of MVIC. Single-fiber absolute and specific force were 0.88 ± 0.19 mN and 114 ± 10 kN/m^2 for myosin heavy chain (MyHC) I and 0.74 ± 0.23 mN and 171 ± 23 kN/m^2 for MyHC IIa fibers. Less than 1% of fibers were positive for the denervation marker neural cell adhesion molecule (NCAM), no fibers expressed embryonic MyHC, and ∼1% of MyHC II fibers expressed neonatal MyHC. In vivo muscle size, force, power, and fatigability were largely within the range for individuals one decade younger. MU behavior was comparable with individuals 20 yr younger. MyHC I fibers produced greater absolute force than reported in untrained young females and females in their eighth decade, whereas MyHC II fiber force was lower because of smaller fiber size. Denervation markers were less prevalent than typically reported at this age. Collectively, these findings illustrate the heterogeneous effects of aging on different features of neuromuscular function, even in an elite older female sprint athlete.

NEW & NOTEWORTHY We report in vivo neuromuscular function, single-fiber mechanics, and denervation markers in a 91-yr-old female who holds the W90$^+$ 200 m world record. Despite reduced muscle size, force, and power, as well as pronounced fast-fiber atrophy, markers of denervation were similar to those in young females and single-fiber force in slow fibers was preserved. Together, these data highlight the differential effects of lifelong sprint training and aging on neural versus muscular components of the neuromuscular system.

aging; human physiology; master athletes; neuromuscular function; sprint world record performance

INTRODUCTION

The aging process is accompanied by a progressive decline in neuromuscular function that compromises the ability of older adults to maintain mobility and functional independence. Age-related reductions in muscle strength, and especially power, occur more rapidly than the loss of skeletal muscle mass, indicating that impairments at multiple locations along the motor pathway contribute to this functional decline (1–3). This problem is further exacerbated by the increased fatigability observed in older adults during high-intensity dynamic contractions (4, 5). In this context, sprint running represents an extreme physiological challenge to the neuromuscular system of older adults,

*C. W. Sundberg and M. V. Franchi contributed equally to this work.
Correspondence: M. V. Franchi (martino.franchi@unipd.it); C. W. Sundberg (csundberg2@medicine.wisc.edu).
Submitted 25 March 2026 / Revised 3 April 2026 / Accepted 29 April 2026

8750-7587/26 Copyright © 2026 The Authors. Licensed under Creative Commons Attribution CC-BY-NC 4.0.
Published by the American Physiological Society.

Downloaded from journals.physiology.org/journal/jappl (130.192.232.211) on November 2, 2026.

requiring rapid force production, high-velocity muscle contractions, and the ability to sustain mechanical output while resisting fatigue (6, 7). Accordingly, world-class master sprinters can provide a unique model to examine the upper limits of neuromuscular preservation with aging. Against this backdrop, the performance of a 91-yr-old female athlete who set a new W90$^+$ world record in the outdoor 200 m event in June 2024 offers an exceptional opportunity to characterize the neuromuscular determinants that support elite sprint performance in the tenth decade of life.

Sprint performance is supported by two complementary physiological "halves of the coin." One half reflects the metabolic determinants, including the integrated function of the oxygen transport cascade and the metabolic pathways necessary to rapidly resynthesize ATP while minimizing disruptions in metabolic homeostasis that contribute to fatigue (8–10). The other half reflects the neuromuscular determinants necessary to generate repeated, rapid, high-force contractions, and the underlying skeletal muscle characteristics that support these functions (6, 7). Importantly, these two halves are highly interconnected, and the metabolic determinants were presented from this athlete in a companion article (11), whereas the neuromuscular determinants are examined in the present study.

Multiple factors along the pathway from the brain to the muscle contribute to the rapid force production required for sprint performance, each of which can be adversely affected by aging (2). For instance, aging can be accompanied by altered motor unit recruitment and firing rates (12), progressive motor neuron loss, and cycles of denervation and collateral reinnervation, which together may compromise the ability to generate rapid, high-force contractions needed for sprinting (2, 13, 14). Structurally, age-related alterations in muscle architecture, such as shorter fascicles and smaller pennation angles, may further limit maximal force and power output (15, 16). At the cellular level, sprint performance relies heavily on fast myosin heavy chain (MyHC) II muscle fibers, which are critical for explosive contractions and are well-known to undergo preferential atrophy during the aging process (17). Although the size-specific force and normalized power of the remaining fast fibers may be preserved with aging (18–20), reductions in total type II fiber area can still have a profound impact on whole-muscle force and power production (21). Collectively, these neural and muscular alterations with age characterize the neuromuscular "half of the sprinting coin," yet the extent to which these determinants can be preserved in an elite sprint athlete in the tenth decade of life, particularly in females, remains largely unknown.

Therefore, the aim of this study was to comprehensively characterize the in vivo and ex vivo neuromuscular profile of a 91-yr-old female world-record sprinter. Through an in-depth evaluation of muscle architecture, neuromuscular function, fatigability, single fiber mechanics, and intramuscular denervation markers, we sought to identify physiological features that may underpin her elite sprint performance in very old age. These data may provide unique insight into the factors limiting human neuromuscular performance, and the potential role of lifelong sprint training in preserving functional capacity during advanced aging.

METHODS

A 91-yr-old female (weight: 58 kg; height: 155 cm; body mass index: 23.9 kg/m^2) who set the W90$^+$ world records in the 200 m outdoor, and 60, 200, and 400 m indoor sprints volunteered to participate in this study. At the time of assessment, she held W90$^+$ world records in the 60 m indoor (13.91 s; March 20, 2024), 200 m indoor (51.08 s; March 10, 2024), 400 m indoor (126.04 s; March 19, 2024), and 200 m outdoor (50.33 s; June 2, 2024). Exercise history was obtained via interview. She began sprint training at ∼20 yr of age, had an ∼15 yr interruption in competition between ages 30 and 45 yr, and subsequently resumed ∼45 yr of structured sprint training up to the time of assessment. The athlete trains at least three times per week, with sessions typically beginning with 2–3 min of light jogging followed by several 50–60 m accelerations at ∼50% of maximal speed. More intense sessions include repeated 50–60 m sprints at ∼80% of maximal speed with ∼3-min of recovery between bouts, and occasionally longer repetitions up to 400 m with 7–8 min of recovery. In the week preceding competition, she increases intensity, performing 200 m runs near maximal speed. Her training is not rigidly structured and is adjusted based on perceived readiness, alternating between slow runs, moderate efforts, and maximal sprints, while a training partner tracks her time.

Experimental Design

All in vivo experiments were performed 1 mo after her indoor world record and 15 days before her outdoor world record in May 2024. The athlete volunteered to participate in the "Trajectory-Age" study (22) and was informed about the aims and potential risks before providing written informed consent. The study conforms to the principles in the Declaration of Helsinki, is registered at ClinicalTrials.gov (NCT06168591), and was approved by the AVEN Ethical Committee (Emilia Romagna region, Italy; Protocol No. 28022; Study ID 283/2022/SPER/UNIPR).

Muscle Architecture

Quadriceps femoris cross-sectional area (CSA) was assessed at 20, 30, 40, 50, and 60% of femur length (distal to proximal) using panoramic ultrasound imaging (Mindray Bio-Medical Electronics, China) (23). CSA was determined by tracing muscle contours with the freehand tool in ImageJ software (v1.52; National Institutes of Health, Bethesda, MD), as described previously (24). Mean quadriceps and vastus lateralis CSA were calculated by averaging CSA values across the measured muscle regions. Vastus lateralis muscle architecture was evaluated using B-mode longitudinal ultrasound scans obtained with a 38 mm probe at 30% and 50% of femur length (25). Fascicle length was determined using the manual linear extrapolation method, whereby visible fascicles were extended with straight lines across the nonvisible portion of the muscle until the projected line intersected the superficial aponeurosis (23, 26, 27). Fascicle length and pennation angle were calculated as the mean of three fascicles analyzed in ImageJ. Vastus lateralis

Downloaded from journals.physiology.org/journal/jappl (130.192.232.211) on November 2, 2026.

muscle thickness was measured as the perpendicular distance between the superficial and deep aponeuroses at the distal, middle, and proximal portions of the image, and the mean of these three values was used for analysis.

Motor Unit Behavior

High-density surface electromyography (HD-EMG) was recorded from the vastus lateralis during trapezoidal isometric contractions performed to 30% and 50% of maximal voluntary isometric contraction (MVIC), with a 2% MVIC·s^{-1} rate of torque increase followed by a 10 s constant-torque plateau at the target level. Muscle activity was recorded using a 64-electrode grid (8 × 8 layout; 10 mm interelectrode distance in the column direction and 20 mm in the row direction; and 70 × 140 mm recording area). The grid was positioned over the muscle belly such that the midpoint of the femur was located between columns 2 and 3, with the rows aligned to the fascicle orientation identified via ultrasound. Monopolar signals were acquired using a wireless system (MEACS, ReC Bioengineering and LISiN, Politecnico di Torino) and synchronized post hoc with torque signals from the Humac Norm via external trigger pulses (28).

HD-EMG signals were band-pass filtered (20–400 Hz) using a fourth-order Butterworth filter. Motor unit firing patterns were extracted using a deconvolutive blind source separation technique (29) and manually edited according to established guidelines (30). Motor unit behavior was characterized by recruitment threshold, mean discharge rate, and the coefficient of variation of discharge rate during the constant-torque phase at both 30% and 50% MVIC, as well as derecruitment threshold for all identified motor units. Torque signals were low-pass filtered at 100 Hz (fourth-order Butterworth), and torque steadiness was quantified as the coefficient of variation during the constant-torque phase.

Maximal Voluntary Isometric Contraction Torque

The participant was seated upright in a Humac Norm dynamometer (Humac Norm 64 bit, CSMI, Stoughton, Massachusetts) with knee and hip angles at 90° (180° corresponding to full extension) and secured to the backrest with chest straps. The dynamometer was positioned so that the axis of rotation of the lever arm was aligned with the axis of rotation of the participant's knee, and the lower leg was secured to the lever arm using a noncompliant strap placed immediately proximal to the malleoli. To ensure that the measured torques and velocities were generated primarily by the knee extensor muscles, the participant was instructed not to grasp any part of the dynamometer with her hands. After a series of submaximal isometric contractions, three maximal MVICs were performed. For each MVIC, the participant was instructed to push "as hard as possible" for 4 s without an earlier countermovement, with 1 min of rest between contractions. MVIC torque was defined as the highest torque achieved over any 250 ms interval. Isometric force was assessed before and immediately after a dynamic fatiguing exercise (see *Dynamic Fatiguing Exercise*). Data were analyzed offline using LabChart software (LabChart software v8, ADInstrument NZ Limited, Dunedin, New Zealand).

Dynamic Fatiguing Exercise

Ten minutes after the baseline MVIC assessment, the participant performed maximal-velocity knee extensions against a load corresponding to 20% of MVIC applied by the dynamometer. The participant was instructed to kick "as fast as possible" once every 3 s for 4 min (80 contractions) (4, 31). Strong verbal encouragement was provided throughout the test to ensure maximal effort and completion of the full range of motion (from 90° to 180° of knee extension) for each contraction. After each contraction, the participant was instructed to relax, and the limb was passively returned to the starting position by the dynamometer. Muscle torque, angular velocity, and power was sampled at 2,000 Hz and analog-to-digitally converted (PowerLab 26 T, ADInstruments, Dunedin, New Zealand). Baseline power output was defined as the highest average power obtained from five consecutive contractions within the first 10 contractions. Decline in muscle power was quantified by expressing the average power from the final five contractions as a percentage of baseline power output (4).

Muscle Biopsy

As described in the companion paper (11), a resting muscle biopsy was taken from vastus lateralis muscle using a 130 mm (6 in.) Weil–Blakesley rongeur conchotome (NDB-2, Fehling Instruments, GmbH&Co, Germany) under local anesthesia (2% lidocaine) applied to the skin and muscle fascia. A 1.0–1.5 cm incision was made through the skin, subcutaneous tissue, and muscle fascia, and an ∼100 mg tissue sample was harvested. Following collection, samples were carefully cleared of excess blood, adipose tissue, and connective tissue, and then divided for subsequent single-fiber mechanical and histological analyses. The bundle for single-fiber contractile experiments was immediately placed in ice-cold glycerol skinning solution and stored at −20°C for up to 3 wk. The bundle for histological analyses was flash-frozen in liquid nitrogen-cooled isopentane and stored at −80°C until sectioning for immunohistochemistry.

Single Fiber Mechanics

Fibers were prepared as described previously (32). In brief, single-fiber segments between 5 and 10 mm in length were isolated from the biopsy sample and tied to a force transducer (400 A; Aurora Scientific) and a high-speed servomotor (controller 312B; Aurora Scientific) with ∼2–3 mm of the fiber suspended between the two attachment points. Fibers were kept at 16°C with a temperature-controlled Peltier unit in 100 μL relaxing solution for the duration of the experiment, except when transferred briefly to a second Peltier unit containing 100 μL of activating solution set at 20°C (33). Sarcomere length was adjusted to 2.5 μm, and fiber length and diameter were determined as described previously (19). CSA was calculated from the mean fiber diameter, assuming the fiber forms a cylinder when suspended briefly in air (<2 s). After completing experiments, the MyHC composition of each fiber was determined by SDS-PAGE as previously described (32) followed by Sypro Ruby (S12000, Thermo Fisher Scientific) staining according to the manufacturer's instructions. Solutions for the single fiber contractile mechanics experiments were derived from an iterative program using the

Downloaded from journals.physiology.org/journal/jappl (130.192.232.211) on November 2, 2026.

stability constants adjusted for temperature, pH, and ionic strength (34, 35) and contained (in mM) 20 imidazole, 7 EGTA, 4 free Mg ATP, 1 free Mg^{2+}, and 14.5 creatine phosphate. ATP was added as Na_2ATP, Mg as $MgCl_2$, creatine phosphate as Na_2 phosphocreatine, and Ca^{2+} as $CaCl_2$. Inorganic phosphate (P_i) was added as K_2HPO_4 to yield a concentration of 4 mM. The ionic strength of both the activating and relaxing solutions was adjusted to 180 mM with KCl. The pH was adjusted to 7.0 with KOH. The relaxing solution contained negligible amounts of Ca^{2+} (pCa 9.0, where pCa = −log10 [Ca^{2+}]), whereas the activating solution contained saturating levels of Ca^{2+} (pCa 4.5). Glycerol skinning solution was composed of 50% relaxing solution and 50% glycerol (vol/vol).

Immunohistochemistry

Immunohistochemical analyses were performed to assess fiber type-specific denervation markers, including neural cell adhesion molecule (NCAM), embryonic myosin heavy chain (MyHCe), and neonatal myosin heavy chain (MyHCn). Lists of specific antibodies are presented in Supplemental Table S1. Muscle tissue was equilibrated to the cryostat (HM525NX, Thermo Fisher Scientific) temperature of −21°C for ≥30 min, oriented upright and exposed in Neg-50 (Ref. 6502, Epredia), and then cross sectioned at 7 μm with a low-profile disposable microtome blade (Ref. 3053835, Epredia) at a 10° clearance angle. Muscle sections were picked up with Superfrost Plus slides (Ref. 6776214, Epredia), air-dried at room temperature (RT) for ≥1 h, and stored at −80°C until staining. On the day of staining, slides were taken from −80°C, air-dried for ≥30 min at RT, and sections were circled with an ImmEdge pen (H-4000, Vector Laboratories), allowing ≥15 min to air-dry and establish a hydrophobic barrier. After rehydration in a Coplin staining jar with 3 × 5 min washes of 1X phosphate-buffered saline (PBS) at pH 7.4, muscle sections were incubated in a humidified slide stain tray (M918-2, Simport Scientific) with a primary antibody cocktail (Supplemental Table S1) and 1X PBS for 90 min at RT. Muscle sections were then washed in a Coplin staining jar 3 × 5 min each with fresh 1X PBS and subsequently incubated in a secondary antibody cocktail (Supplemental Table S1) and 1X PBS for 60 min at RT. Sections were again washed 3 × 5 min with fresh 1X PBS, mounted with 1:1 at 1X PBS/glycerol (5092-02, Macron Fine Chemicals), and coverslipped with a microcover glass (48393-221, VWR). Coverslips were sealed onto the slides with clear nail polish and then stored at 4°C until imaging. Muscle section images were acquired using a high-resolution fluorescence microscope (BZ-X810, Keyence) with a Plan Apochromat ×20 mounted objective (BZ-PA20, Keyence) and Cy5 (49006, Chroma Technology), FITC/Alexa Fluor 488/Fluo3/Oregon Green (49011, Chroma Technology), and CY3/tetramethylrhodamine isothiocyanate (TRITC; 49004, Chroma Technology). Positive denervation markers were visually identified by two independent investigators and counted in a fiber type-specific manner.

RESULTS

Knee Extensor Muscle Size and Architecture

At 50% of femur length, the CSAs of the vastus lateralis, vastus medialis, vastus intermedius, and rectus femoris were 9.23, 5.76, 17.66, and 3.85 cm^2, respectively. The sum of the CSAs at midfemur was 36.49 cm^2 (Fig. 1*A*). The vastus lateralis fascicle length was 6.7 cm, with a pennation angle of 11.56° and a muscle thickness of 1.4 cm.

Motor Unit Properties

We decomposed 19 motor units from the vastus lateralis, 17 of which were already recruited during the 30% MVIC trial. Individual motor unit firing patterns are shown in Fig. 2, *A*

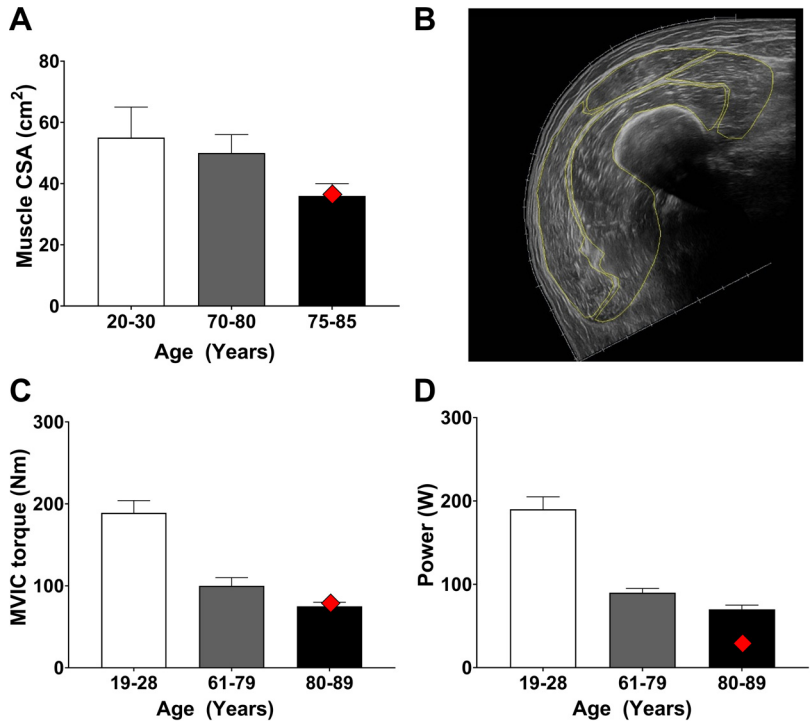


Figure 1. Knee extensor force, power, and cross-sectional area (CSA) of the world record holder compared with reference data. All panels were adapted from the original publications and modified to improve clarity and to incorporate data from the 91-yr-old world record holder (red diamonds). *A*: CSA of the knee extensors at 50% of femur length compared with young (26 ± 5 yr), old (75 ± 4 yr), and old sarcopenic (80 ± 5 yr) males and females previously reported by Sarto et al. (36). *B*: panoramic ultrasound image of the knee extensor muscles at 50% of femur length from the 91-yr-old female world record holder, with the knee extensor muscles highlighted in yellow. *C* and *D*: knee extensor maximal voluntary isometric contraction (MVIC) torque (*C*) and power elicited with a 20% MVIC load (*D*), compared with young (23 ± 2 yr), old (71 ± 6 yr), and very old females (83 ± 3 yr), previously reported by Sundberg et al. (4).

Downloaded from journals.physiology.org/journal/jappl (130.192.232.211) on November 2, 2026.

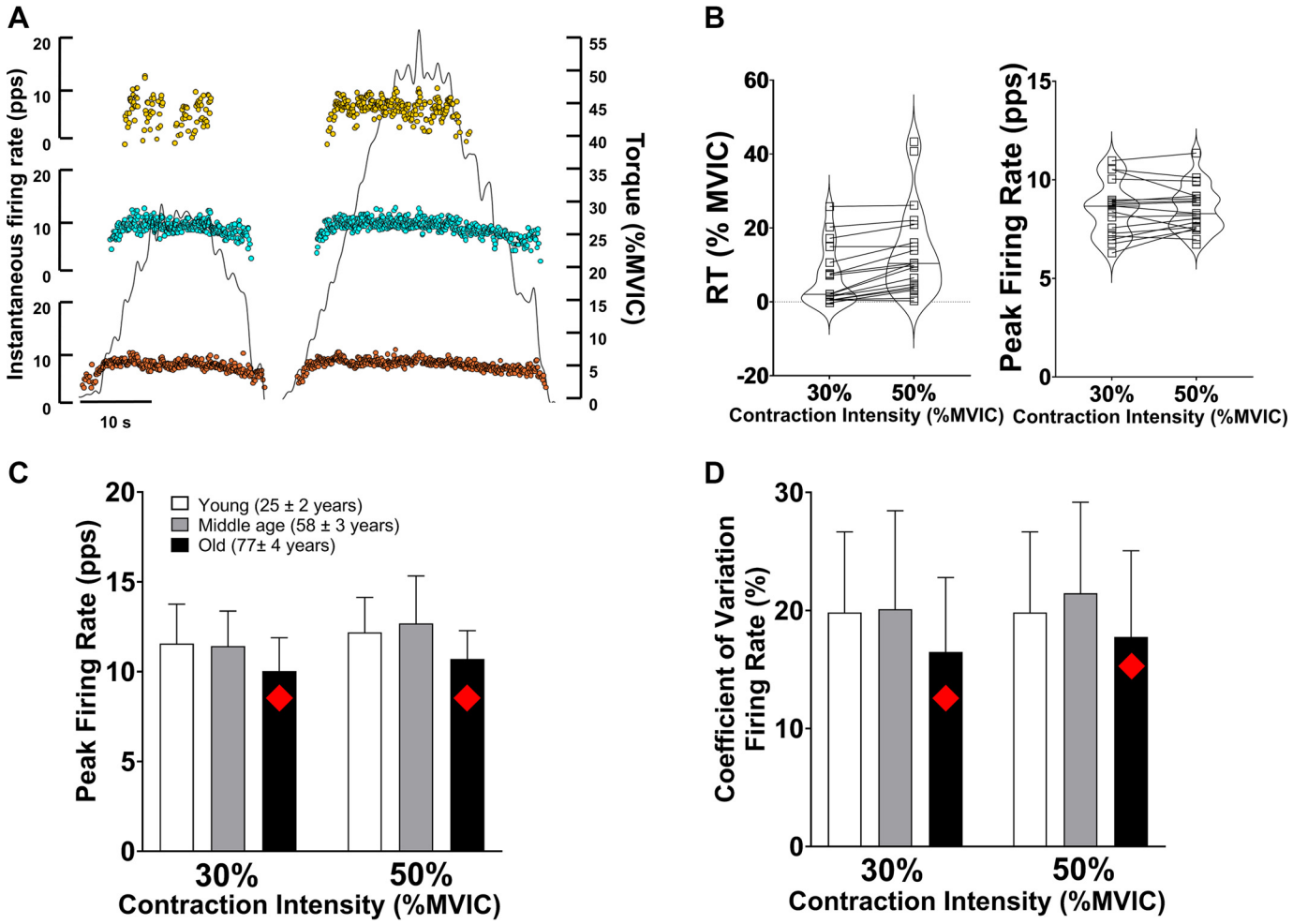


Figure 2. Motor unit behavior. All panels were adapted from the original publication and modified to improve clarity and incorporate data from the 91-yr-old world record holder (red diamonds). *A*: representative instantaneous firing rates from three motor units of the world record holder during contractions at 30% (*left*) and 50% (*right*) MVIC. The same motor units were tracked across both contractions. *B*: recruitment threshold (RT) and peak firing rate of all motor units were identified and tracked between 30% ($n = 17$) and 50% ($n = 19$) MVIC in the world record holder. Peak firing rate (*C*) and coefficient of variation of firing rate during trapezoidal isometric knee extensor contractions at 30% and 50% MVIC (*D*). *C* and *D*: mean data from the 91-yr-old world record holder are compared with young ($n = 5$, 25 ± 2 yr), middle-aged ($n = 29$, 58 ± 3 yr), and older ($n = 11$, 77 ± 4 yr) females from the study by Carbonaro et al. (12). MVIC, maximal voluntary isometric contraction.

and *B*. The recruitment threshold was 12 ± 11% MVIC, and the derecruitment threshold was 11 ± 8% MVIC, resulting in a delta threshold of −2 ± 7%. Torque steadiness, expressed as the coefficient of variation (CV), was 5% and 4% during contractions at 30% and 50% MVIC, respectively. Over the same time window, the CV of motor unit firing rate was 12% at 30% MVIC and 15% at 50% MVIC (Fig. 2*D*). Peak motor unit firing rates were similar between contraction intensities (8.5 ± 1.4 pps at 30% MVIC and 8.5 ± 1.2 pps at 50% MVIC, respectively; Fig. 2*C*).

Neuromuscular Function and Fatigability

Knee extensor MVIC torque was 79 Nm (Fig. 1*C*) and declined by 23% after the fatiguing exercise (60 Nm). MVIC torque normalized to CSA was 2.16 $Nm \cdot cm^{-2}$. Initial knee extensor power was 28 W (Fig. 1*D*) and decreased by 43% by the end of the fatiguing exercise (16 W). Similarly, angular velocity declined by 34% (from 101 to 67° $\cdot s^{-1}$), whereas torque remained relatively constant throughout the fatiguing exercise (from 14 to 13 Nm).

Single-Fiber Mechanics

Results from single-fiber mechanics are presented in Fig. 3. A total of 33 fibers were analyzed, including 12 MyHC I, 17 MyHC IIa, 2 MyHC I/IIa, and 2 MyHC IIa/IIx fibers. MyHC I fibers had a mean CSA of 7,676 ± 1,662 μm^2 (Fig. 3*A*) and produced an average absolute force of 0.88 ± 0.19 mN (Fig. 3*B*), resulting in a size-specific force of 114 ± 10 $kN \cdot m^{-2}$ (Fig. 3*C*). MyHC IIa fibers had a mean CSA of 4,313 ± 1,220 μm^2 (Fig. 3*A*) and produced an average absolute force of 0.74 ± 0.23 mN (Fig. 3*B*), resulting in a size-specific force of 171 ± 23 $kN \cdot m^{-2}$ (Fig. 3*C*). Although only 2 MyHC I/IIa fibers were studied, they had a mean CSA of 3,937 ± 1,473 μm^2 and produced an average absolute force of 0.47 ± 0.23 mN, resulting in a size-specific force of 113 ± 17 $kN \cdot m^{-2}$. Similarly, only 2 MyHC IIa/IIx fibers were studied, which had a mean CSA of 651 ± 367 μm^2 and produced an average absolute force of 0.11 ± 0.07 mN, resulting in a size-specific force of 150 ± 22 $kN \cdot m^{-2}$.

Downloaded from journals.physiology.org/journal/jappl (130.192.232.211) on November 2, 2026.

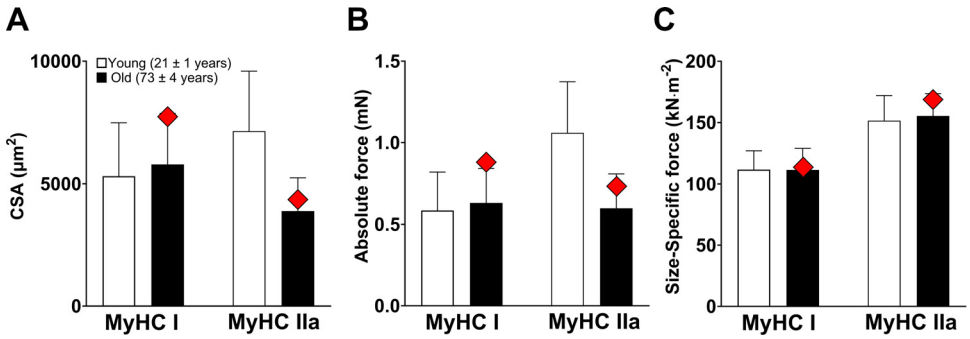


Figure 3. Single-fiber cross-sectional area (CSA), peak force, and size-specific force of myosin heavy chain (MyHC) I and IIa fibers from the world record holder compared with reference data. All panels were adapted from the original publication and modified to improve clarity and to incorporate data from the 91-yr-old world record holder (red diamonds). Mean data from 12 MyHC I and 17 MyHC IIa fibers from the world record holder are compared with single fiber data from young ($n = 5$, 21±1 yr, 69 fibers) and older ($n = 7$, 73±4 yr, 103 fibers) females previously reported by Teigen et al. (20). Single fiber CSA (*A*), absolute force (*B*), and size-specific force (*C*) of MyHC I and IIa fibers.

Muscle Denervation Markers

Muscle denervation marker data are presented in Fig. 4. Fewer than 1% of both MyHC I and MyHC II fibers were positive for the denervation marker NCAM (1 of 187 MyHC I fibers and 1 of 248 MyHC II fibers; Fig. 4*A*). No fibers were positive for MyHCe (Fig. 4*C*). In addition, no MyHC I fibers were positive for MyHCn, whereas ~1% of MyHC II fibers were MyHCn-positive (3 of 282 fibers; Fig. 4*D*).

DISCUSSION

This case study constitutes the other "half of the coin" of a broader investigation aimed at comprehensively characterizing the physiological profile of a 91-yr-old female sprint athlete who, in 2024, broke the world record for the 200 m sprint in the W90^{+} age category. To our knowledge, this is the first study to provide an integrated assessment of neuromuscular function, fatigability, single fiber mechanics, and intramuscular denervation markers in a female world record holder in her tenth decade of life. The principal findings were: *1*) clear evidence of age-related muscle atrophy and typical alterations in muscle architecture, accompanied by reduced whole muscle force and power; *2*) fatigability comparable with females in their 80s (4), *3*) motor unit recruitment behavior similar to that observed in females in their 70s (12); *4*) remarkably large and strong MyHC I fibers, along with lower force production in MyHC IIa fibers due primarily

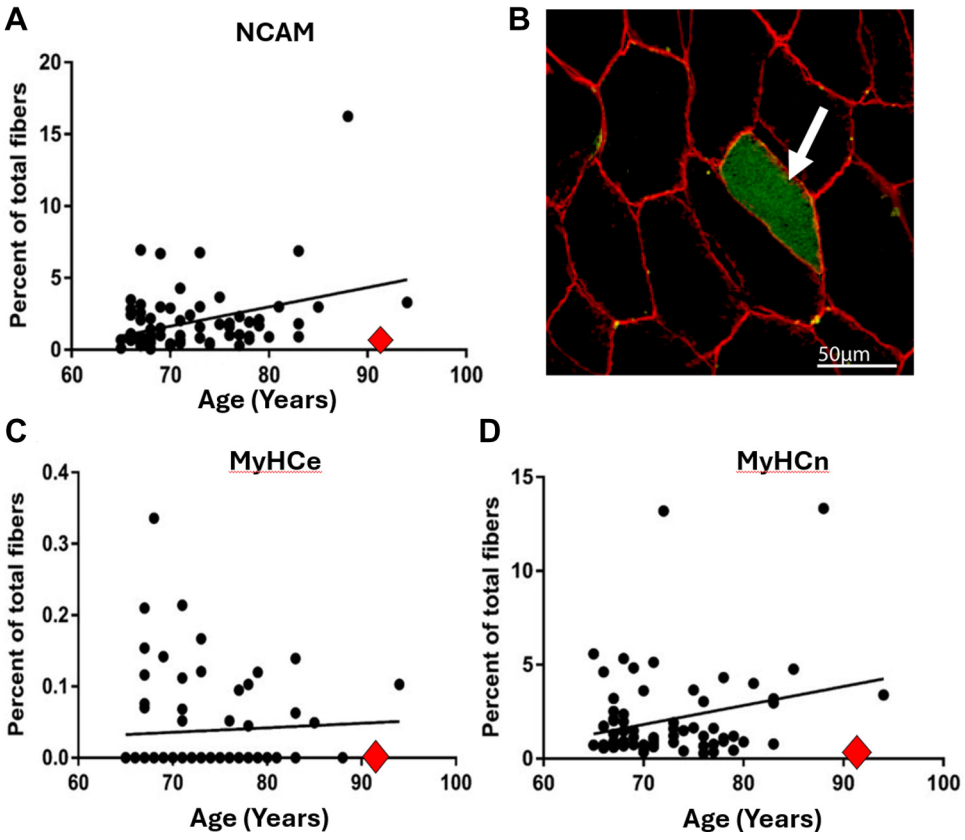


Figure 4. Denervation markers in the world record holder compared with reference data. All panels were adapted from the original publication by Soendenbroe et al. (37) with permission and modified to improve clarity and to incorporate data from the 91-yr-old world record holder (red diamonds). *A*: neural cell adhesion molecule (NCAM). *B*: representative image from the world record holder demonstrating an NCAM-positive fiber (green, white arrow) with dystrophin labeling the fiber borders (red). *C*: embryonic myosin heavy chain (MyHCe). *D*: neonatal myosin heavy chain (MyHCn).

Downloaded from journals.physiology.org/journal/jappl (130.192.232.211) on November 2, 2026.

to their smaller size; and *5*) minimal evidence of intramuscular denervation. These findings suggest that lifelong sprint training may help preserve muscle innervation and maintain key aspects of neuromuscular function at levels that resemble those of individuals 10–20 yr younger, despite pronounced age-related atrophy of fast fibers.

Neuromuscular Function and Whole Muscle Morphology

The in vivo neuromuscular function assessments indicated that the world record holder's knee extensor maximal voluntary isometric contraction torque, power output, and fatigability were comparable to values reported from females in their 80s (4, 36). Similarly, her muscle architecture measured via ultrasound, including CSA (Fig. 1*A*), fascicle length, pennation angle, and thickness, was comparable to that of males and females in their 80s with sarcopenia (36, 38). These findings suggest that, in contrast to the preserved muscle oxidative capacity reported in the companion paper (11), her knee extensor muscles exhibited hallmark features of advanced age-related atrophy and reduced whole-muscle function. However, it is important to note that we were unable to directly compare her data with those of other females in their tenth decade of life (39). Thus, despite clear evidence of age-related decline, her neuromuscular and architectural characteristics appear broadly comparable to those of individuals one to two decades younger. This is particularly notable given evidence that declines in skeletal muscle mass and function appear to accelerate during the very late stages of life and may differ in females compared with males (39–43).

Motor unit behavior exhibited features consistent with typical aging (12). During sustained isometric contractions at 30% MVIC, the world record holder's coefficient of variation of motor unit firing rate was similar to values typically reported in older females (12, 44), indicating that her motor unit discharge patterns, neural control, and synaptic noise are comparable with those observed in females in their 70s (12, 45). Similarly, at higher contraction intensities (50% MVIC), both firing rate variability and force steadiness were also comparable with values observed in males and females approximately two decades younger (12, 44). In addition, motor unit recruitment thresholds appeared lower than those commonly observed in older males and females, suggesting earlier and more complete recruitment followed by rapid derecruitment, without the prolonged activation patterns reported in individuals in their 70s (12, 46). These findings indicate that the world record holder's motor unit behavior and neuromuscular control resemble those of males and females ~20 yr younger.

Muscle Fiber Properties

Single-fiber mechanics analyses largely demonstrated the expected fiber type-specific differences associated with aging (Fig. 3). Specifically, her MyHC IIa fibers produced absolute force comparable with those of older females in their 70s but lower than those of younger females in their 20s, whereas her MyHC I fibers generated ~30% greater absolute force than those of both young and older females (20). After normalizing for fiber size, these differences were largely eliminated, with MyHC I fiber-specific force similar to both young and older females, whereas type II fibers demonstrated slightly higher specific force compared with both age groups (20). These findings support the concept that age-related reductions in absolute force production in fast fibers are driven primarily by reductions in fiber size, whereas intrinsic force-generating capacity is largely preserved with advanced age (18–20, 47). In addition, minimal evidence of denervation markers was observed (Fig. 4) compared with what is typically expected in the tenth decade of life (37). This suggests that reinnervation processes may remain active even beyond ~75 yr of age, a period during which denervation is thought to surpass reinnervation in most individuals (48, 49). It is possible that denervation may have occurred earlier in life, with affected fibers lost prior to sampling; however, due to the lack of data on denervation trajectories in females in their 90s, the timing of these processes remains uncertain. Notably, other commonly reported features of denervation, such as MyHC I fiber grouping and centralized nuclei (~1%, 4 of 363 fibers), were not readily apparent in this athlete. These findings suggest that lifelong sprint training may help preserve intrinsic fiber force-generating capacity and maintain muscle fiber innervation status, even into the tenth decade of life.

Conclusions

This case study illustrates that a lifelong commitment to sprint training may meaningfully influence the trajectory of neuromuscular aging. Although age-related structural remodeling of skeletal muscle and declines in muscle mass, maximal force, and power production appear unavoidable, the world record holder exhibited preserved intrinsic contractile function at the single-fiber level and evidence of maintained muscle innervation status. When interpreted alongside the companion paper demonstrating preservation of oxidative capacity and key components of the oxygen transport cascade (11), these findings suggest that the maintenance of mitochondrial bioenergetics and muscle innervation may be key determinants of exceptional sprint performance in the tenth decade of life. In contrast, age-related alterations in muscle architecture and reductions in fast fiber absolute force and cross-sectional area likely represent important limiting factors in this athlete. Collectively, these results highlight the potential for lifelong sprint training to attenuate age-related declines across multiple physiological systems and to preserve functional capacity well into very advanced age.

DATA AVAILABILITY

Data will be made available upon reasonable request.

SUPPLEMENTAL MATERIAL

Supplemental Table S1: https://doi.org/10.6084/m9.figshare.31852552.

ACKNOWLEDGMENTS

All the authors deeply thank Emma Maria Mazzenga for her precious time and effort. Moreover, we sincerely thank Prof. La

Downloaded from journals.physiology.org/journal/jappl (130.192.232.211) on November 2, 2026.

Torre Antonio for the fundamental help in creating this incredible collaboration and to Andrea Pilotto for the contribution to the logistical organization. Antibody BA-D5 was deposited to the DSHB by S. Schiaffino, F1.652 was deposited to the DSHB by H. M. Blau, and MANDYS1(3B7) was deposited to the DSHB by G. E. Morris.

GRANTS

This work was supported by Ministero dell'Istruzione, dell'Università e della Ricerca (MIUR) Trajector-AGE (2020477RW5) and ReActiveAGE (P2022FNCPR) projects of National Interest (Italy) (to M.V.F. and S.P.), and a National Institutes of Health Grant R01 AG048262 (to C.W.S.).

DISCLOSURES

No conflicts of interest, financial or otherwise, are declared by the authors.

AUTHOR CONTRIBUTIONS

S.P., M.V.F., and C.W.S. conceived and designed research; M.C., I.D., L.E.T., M.C., M.A., M.G., C.M.B., S.P., M.V.F., and C.W.S. performed experiments; M.C., I.D., L.E.T., M.C., M.A., M.G., C.M.B., M.C., S.P., M.V.F., and C.W.S. analyzed data; M.C., S.P., M.V.F., and C.W.S. interpreted results of experiments; M.C. and C.W.S. prepared figures; M.C. and C.W.S. drafted manuscript; M.C., I.D., L.E.T., M.C., M.A., M.G., C.M.B., M.C., R.B., A.B., S.P., M.V.F., and C.W.S. edited and revised manuscript; M.C., I.D., L.E.T., M.C., M.A., M.G., C.M.B., M.C., R.B., A.B., S.P., M.V.F., and C.W.S. approved final version of manuscript.

REFERENCES

1. **Korhonen MT**, **Cristea A**, **Alén M**, **Häkkinen K**, **Sipilä S**, **Mero A**, **Viitasalo JT**, **Larsson L**, **Suominen H.** Aging, muscle fiber type, and contractile function in sprint-trained athletes. *J Appl Physiol (1985)* 101: 906–917, 2006. doi:10.1152/japplphysiol.00299.2006.
2. **Hunter SK**, **Pereira HM**, **Keenan KG.** The aging neuromuscular system and motor performance. *J Appl Physiol (1985)* 121: 982–995, 2016. doi:10.1152/japplphysiol.00475.2016.
3. **Girts RM**, **Mota JA**, **Harmon KK**, **MacLennan RJ**, **Stock MS.** Vastus lateralis motor unit recruitment thresholds are compressed towards lower forces in older men. *J Frailty Aging* 9: 191–196, 2020. doi:10.14283/jfa.2020.19.
4. **Sundberg CW**, **Kuplic A**, **Hassanlouei H**, **Hunter SK.** Mechanisms for the age-related increase in fatigability of the knee extensors in old and very old adults. *J Appl Physiol (1985)* 125: 146–158, 2018. doi:10.1152/japplphysiol.01141.2017.
5. **Paris MT**, **McNeil CJ**, **Power GA**, **Rice CL**, **Dalton BH.** Age-related performance fatigability: a comprehensive review of dynamic tasks. *J Appl Physiol (1985)* 133: 850–866, 2022. doi:10.1152/japplphysiol.00319.2022.
6. **Bishop D**, **Girard O**, **Mendez-Villanueva A.** Repeated-sprint ability – part II: recommendations for training. *Sports Med* 41: 741–756, 2011. doi:10.2165/11590560-000000000-00000.
7. **Girard O**, **Mendez-Villanueva A**, **Bishop D.** Repeated-sprint ability – part I: factors contributing to fatigue. *Sports Med* 41: 673–694, 2011. doi:10.2165/11590550-000000000-00000.
8. **Sundberg CW**, **Fitts RH.** Bioenergetic basis of skeletal muscle fatigue. *Curr Opin Physiol* 10: 118–127, 2019. doi:10.1016/j.cophys.2019.05.004.
9. **Bundle MW**, **Hoyt RW**, **Weyand PG.** High-speed running performance: a new approach to assessment and prediction. *J Appl Physiol (1985)* 95: 1955–1962, 2003. doi:10.1152/japplphysiol.00921.2002.
10. **Bundle MW**, **Weyand PG.** Sprint exercise performance. *Exerc Sport Sci Rev* 40: 174–182, 2012. doi:10.1097/JES.0b013e318258e1c1.
11. **Colosio M**, **Pilotto AM**, **Ansaldo M**, **Dobrzycki I**, **Pellegrino MA**, **Bottinelli R**, **Re R**, **Botter A**, **Franchi MV**, **Sundberg CW**, **Porcelli S.** One half of the sprinting coin: the oxygen transport cascade of a 91-year-old female world-record sprinter. *J Appl Physiol* (1985). In press. doi:10.1152/japplphysiol.00279.2026.
12. **Carbonaro M**, **Boccardo M**, **Brusco CM**, **Pilotto AM**, **Re R**, **Lauretani F**, **Porcelli S**, **Franchi MV**, **Botter A.** Motor unit behaviour adaptations across the lifespan: sex differences in young, middle-aged and old adults (Preprint). *bioRxiv* 2025. doi:10.64898/2025.12.19.695460.
13. **Enoka RM**, **Duchateau J.** Translating fatigue to human performance. *Med Sci Sports Exerc* 48: 2228–2238, 2016. doi:10.1249/MSS.0000000000000929.
14. **Janssen I**, **Heymsfield SB**, **Ross R.** Low relative skeletal muscle mass (sarcopenia) in older persons is associated with functional impairment and physical disability. *J Am Geriatr Soc* 50: 889–896, 2002. doi:10.1046/j.1532-5415.2002.50216.x.
15. **Goodpaster BH**, **Park SW**, **Harris TB**, **Kritchevsky SB**, **Nevitt M**, **Schwartz AV**, **Simonsick EM**, **Tylavsky FA**, **Visser M**, **Newman AB.** The loss of skeletal muscle strength, mass, and quality in older adults: the health, aging and body composition study. *J Gerontol A Biol Sci Med Sci* 61: 1059–1064, 2006. doi:10.1093/gerona/61.10.1059.
16. **Narici MV**, **Maffulli N.** Sarcopenia: characteristics, mechanisms and functional significance. *Br Med Bull* 95: 139–159, 2010. doi:10.1093/bmb/ldq008.
17. **Nilwik R**, **Snijders T**, **Leenders M**, **Groen BBL**, **van Kranenburg J**, **Verdijk LB**, **van Loon LJC.** The decline in skeletal muscle mass with aging is mainly attributed to a reduction in type II muscle fiber size. *Exp Gerontol* 48: 492–498, 2013. doi:10.1016/j.exger.2013.02.012.
18. **Grosicki GJ**, **Zepeda CS**, **Sundberg CW.** Single muscle fibre contractile function with ageing. *J Physiol* 600: 5005–5026, 2022. doi:10.1113/JP282298.
19. **Teigen LE**, **Sundberg CW**, **Kelly LJ**, **Hunter SK**, **Fitts RH.** Ca^{2+} dependency of limb muscle fiber contractile mechanics in young and older adults. *Am J Physiol Cell Physiol* 318: C1238–C1251, 2020. doi:10.1152/ajpcell.00575.2019.
20. **Teigen LE**, **Zepeda CS**, **Dobrzycki I**, **Hunter SK**, **Fitts RH**, **Sundberg CW.** Effects of acidosis and inorganic phosphate on Ca^{2+} sensitivity of young and older adult skeletal muscle fibers. *Am J Physiol Cell Physiol* 330: C224–C237, 2026. doi:10.1152/ajpcell.00445.2025.
21. **Horwath O**, **Moberg M**, **Edman S**, **Philp A**, **Apró W.** Ageing leads to selective type II myofibre deterioration and denervation independent of reinnervative capacity in human skeletal muscle. *Exp Physiol* 110: 277–292, 2025. doi:10.1113/EP092222.
22. **Lauretani F**, **Maggio M**, **Pilotto AM**, **Ansaldo M**, **Brusco CM**, **Carbonaro M**, **Amendola C**, **Nabacino M**, **Testa C**, **Ciuni A**, **Sverzellati N**, **Zucchini I**, **Salvi M**, **Mastropietro A**, **Re R**, **Botter A**, **Franchi MV**, **Porcelli S.** The trajectories of neuromuscular aging (TRAJECTOR AGE Clinical Trial): study rationale and methodological protocol. *J Am Geriatr Soc* 73: 2819–2827, 2025. doi:10.1111/jgs.70005.
23. **Monti E**, **Franchi MV**, **Badiali F**, **Quinlan JI**, **Longo S**, **Narici MV.** The time-course of changes in muscle mass, architecture and power during 6 weeks of plyometric training. *Front Physiol* 11: 946, 2020. doi:10.3389/fphys.2020.00946.
24. **Franchi MV**, **Badiali F**, **Sarto F**, **Müller P**, **Müller NG**, **Rehfeld K**, **Monti E**, **Rankin D**, **Longo S**, **Lund J**, **Hökelmann A**, **Narici M.** Neuromuscular aging: a case for the neuroprotective effects of dancing. *Gerontology* 69: 73–81, 2023. doi:10.1159/000524843.
25. **Narici M**, **McPhee J**, **Conte M**, **Franchi MV**, **Mitchell K**, **Tagliaferri S**, **Monti E**, **Marcolin G**, **Atherton PJ**, **Smith K**, **Phillips B**, **Lund J**, **Franceschi C**, **Maggio M**, **Butler-Browne GS.** Age-related alterations in muscle architecture are a signature of sarcopenia: the ultrasound sarcopenia index. *J Cachexia Sarcopenia Muscle* 12: 973–982, 2021. doi:10.1002/jcsm.12720.
26. **Brusco CM**, **Pinto RS**, **Blazevich AJ.** Reliability and comparison of sonographic methods for in vivo measurement of human biceps femoris long-head architecture. *Med Sci Sports Exerc* 54: 2216–2226, 2022. doi:10.1249/MSS.0000000000003015.
27. **Franchi MV**, **Fitze DP**, **Raiteri BJ**, **Hahn D**, **Spörri J.** Ultrasound-derived biceps femoris long head fascicle length: extrapolation pitfalls. *Med Sci Sports Exerc* 52: 233–243, 2020. doi:10.1249/MSS.0000000000002123.

Downloaded from journals.physiology.org/journal/jappl (130.192.232.211) on November 2, 2026.

28. **Cerone GL**, **Giangrande A**, **Ghislieri M**, **Gazzoni M**, **Piitulainen H**, **Botter A.** Design and validation of a wireless body sensor network for integrated EEG and HD-sEMG acquisitions. *IEEE Trans Neural Syst Rehabil Eng* 30: 61–71, 2022. doi:10.1109/TNSRE.2022.3140220.
29. **Negro F**, **Muceli S**, **Castronovo AM**, **Holobar A**, **Farina D.** Multi-channel intramuscular and surface EMG decomposition by convolutive blind source separation. *J Neural Eng* 13: 026027, 2016. doi:10.1088/1741-2560/13/2/026027.
30. **Del Vecchio A**, **Holobar A**, **Falla D**, **Felici F**, **Enoka RM**, **Farina D.** Tutorial: analysis of motor unit discharge characteristics from high-density surface EMG signals. *J Electromyogr Kinesiol* 53: 102426, 2020. doi:10.1016/j.jelekin.2020.102426.
31. **Wrucke DJ**, **Colosio M**, **James JJ**, **Hunter SK**, **Sundberg CW.** Initial contractions of a single-load fatiguing exercise provide a valid assessment of age-related differences in peak power. *J Appl Physiol (1985)* 140: 1320–1328, 2026. doi:10.1152/japplphysiol.00159.2026.
32. **Sundberg CW**, **Hunter SK**, **Trappe SW**, **Smith CS**, **Fitts RH.** Effects of elevated H^+ and P_i on the contractile mechanics of skeletal muscle fibres from young and old men: implications for muscle fatigue in humans. *J Physiol* 596: 3993–4015, 2018. doi:10.1113/JP276018.
33. **Nelson CR**, **Debold EP**, **Fitts RH.** Phosphate and acidosis act synergistically to depress peak power in rat muscle fibers. *Am J Physiol Cell Physiol* 307: C939–C950, 2014. doi:10.1152/ajpcell.00206.2014.
34. **Fabiato A.** Computer programs for calculating total from specified free or free from specified total ionic concentrations in aqueous solutions containing multiple metals and ligands. *Methods Enzymol* 157: 378–417, 1988. doi:10.1016/0076-6879(88)57093-3.
35. **Fabiato A**, **Fabiato F.** Calculator programs for computing the composition of the solutions containing multiple metals and ligands used for experiments in skinned muscle cells. *J Physiol (Paris)* 75: 463–505, 1979.
36. **Sarto F**, **Franchi MV**, **McPhee JS**, **Stashuk DW**, **Paganini M**, **Monti E**, **Rossi M**, **Sirago G**, **Zampieri S**, **Motanova ES**, **Valli G**, **Moro T**, **Paoli A**, **Bottinelli R**, **Pellegrino MA**, **De Vito G**, **Blau HM**, **Narici MV.** Neuromuscular impairment at different stages of human sarcopenia. *J Cachexia Sarcopenia Muscle* 15: 1797–1810, 2024. doi:10.1002/jcsm.13531.
37. **Soendenbroe C**, **Heisterberg MF**, **Schjerling P**, **Karlsen A**, **Kjaer M**, **Andersen JL**, **Mackey AL.** Molecular indicators of denervation in aging human skeletal muscle. *Muscle Nerve* 60: 453–463, 2019. doi:10.1002/mus.26638.
38. **Strasser EM**, **Draskovits T**, **Praschak M**, **Quittan M**, **Graf A.** Association between ultrasound measurements of muscle thickness, pennation angle, echogenicity and skeletal muscle strength in the elderly. *Age (Dordr)* 35: 2377–2388, 2013 [Erratum in *Age (Dordr)* 35: 2025–2026, 2013]. doi:10.1007/s11357-013-9517-z.
39. **Suetta C**, **Haddock B**, **Alcazar J**, **Noerst T**, **Hansen OM**, **Ludvig H**, **Kamper RS**, **Schnohr P**, **Prescott E**, **Andersen LL**, **Frandsen U**, **Aagaard P**, **Bülow J**, **Hovind P**, **Simonsen L.** The Copenhagen sarcopenia study: lean mass, strength, power, and physical function in a Danish cohort aged 20-93 years. *J Cachexia Sarcopenia Muscle* 10: 1316–1329, 2019. doi:10.1002/JCSM.12477.
40. **Wilkinson DJ**, **Piasecki M**, **Atherton PJ.** The age-related loss of skeletal muscle mass and function: measurement and physiology of muscle fibre atrophy and muscle fibre loss in humans. *Ageing Res Rev* 47: 123–132, 2018. doi:10.1016/j.arr.2018.07.005.
41. **Gordon EH**, **Peel NM**, **Samanta M**, **Theou O**, **Howlett SE**, **Hubbard RE.** Sex differences in frailty: a systematic review and meta-analysis. *Exp Gerontol* 89: 30–40, 2017. doi:10.1016/j.exger.2016.12.021.
42. **Alcazar J**, **Aagaard P**, **Haddock B**, **Kamper RS**, **Hansen SK**, **Prescott E**, **Alegre LM**, **Frandsen U**, **Suetta C.** Age- and sex-specific changes in lower-limb muscle power throughout the lifespan. *J Gerontol A Biol Sci Med Sci* 75: 1369–1378, 2020. doi:10.1093/gerona/glaa013.
43. **Wrucke DJ**, **Kuplic A**, **Adam MD**, **Hunter SK**, **Sundberg CW.** Neural and muscular contributions to the age-related differences in peak power of the knee extensors in men and women. *J Appl Physiol (1985)* 137: 1021–1040, 2024. doi:10.1152/japplphysiol.00773.2023.
44. **Piasecki J**, **Inns TB**, **Bass JJ**, **Scott R**, **Stashuk DW**, **Phillips BE**, **Atherton PJ**, **Piasecki M.** Influence of sex on the age-related adaptations of neuromuscular function and motor unit properties in elite masters athletes. *J Physiol* 599: 193–205, 2021. doi:10.1113/JP280679.
45. **Tracy BL**, **Maluf KS**, **Stephenson JL**, **Hunter SK**, **Enoka RM.** Variability of motor unit discharge and force fluctuations across a range of muscle forces in older adults. *Muscle Nerve* 32: 533–540, 2005. doi:10.1002/mus.20392.
46. **Guo Y**, **Jones EJ**, **Inns TB**, **Ely IA**, **Stashuk DW**, **Wilkinson DJ**, **Smith K**, **Piasecki J**, **Phillips BE**, **Atherton PJ**, **Piasecki M.** Neuromuscular recruitment strategies of the vastus lateralis according to sex. *Acta Physiol (Oxf)* 235: e13803, 2022. doi:10.1111/apha.13803.
47. **Gries KJ**, **Minchev K**, **Raue U**, **Grosicki GJ**, **Begue G**, **Finch WH**, **Graham B**, **Trappe TA**, **Trappe S.** Single-muscle fiber contractile properties in lifelong aerobic exercising women. *J Appl Physiol (1985)* 127: 1710–1719, 2019. doi:10.1152/japplphysiol.00459.2019.
48. **Hepple RT**, **Rice CL.** Innervation and neuromuscular control in ageing skeletal muscle. *J Physiol* 594: 1965–1978, 2016. doi:10.1113/JP270561.
49. **Sonjak V**, **Jacob K**, **Morais JA**, **Rivera-Zengotita M**, **Spendiff S**, **Spake C**, **Taivassalo T**, **Chevalier S**, **Hepple RT.** Fidelity of muscle fibre reinnervation modulates ageing muscle impact in elderly women. *J Physiol* 597: 5009–5023, 2019. doi:10.1113/JP278261.

Downloaded from journals.physiology.org/journal/jappl (130.192.232.211) on November 2, 2026.